BIOCHEMISTRY
including biophysical chemistry & molecular biology

Article

pubs.acs.org/biochemistry

A Nucleotide-Gated Molecular Pore Selects Sulfotransferase Substrates

Ian Cook,[†] Ting Wang,[†] Charles N. Falany,[‡] and Thomas S. Leyh*[,†]

[†]Department of Microbiology and Immunology, Albert Einstein College of Medicine, 1300 Morris Park Avenue, Bronx, New York 10461-1926, United States

[‡]Pharmacology and Immunology, University of Alabama School of Medicine, 1670 University Boulevard, VH G133M, Birmingham, Alabama 35294-0019, United States

ABSTRACT: Human SULT2A1 is one of two predominant sulfotransferases in liver and catalyzes transfer of the sulfuryl moiety ($-SO_3$) from activated sulfate (PAPS, 3′-phosphoadenosine 5-phosphosulfate) to hundreds of acceptors (metabolites and xenobiotics). Sulfation recodes the biologic activity of acceptors by altering their receptor interactions. The molecular basis on which these enzymes select and sulfonate specific acceptors from complex mixtures of competitors in vivo is a long-standing issue in the SULT field. Raloxifene, a synthetic steroid used in the prevention of osteoporosis, and dehydroepiandrosterone (DHEA), a ubiquitous steroid precusor, are reported to be sulfated efficiently by SULT2A1 in vitro, yet unlike DHEA, raloxifene is not sulfated in vivo. This selectivity was explored in initial rate and equilibrium binding studies that demonstrate pronounced binding antisynergy (21-fold) between PAPS and raloxifene, but not DHEA. Analysis of crystal structures suggests that PAP binding restricts access to the acceptor-binding pocket by restructuring a nine-residue segment of the pocket edge that constricts the active site opening, or "pore", that sieves substrates on the basis of their geometries. In silico docking predicts that raloxifene, which is considerably larger than DHEA, can bind only to the unliganded (open) enzyme, whereas DHEA binds both the open and closed forms. The predictions of these structures with regard to substrate binding are tested using equilibrium and pre-steady-state ligand binding studies, and the results confirm that a nucleotide-driven isomerization controls access to the acceptor-binding pocket and plays an important role in substrate selection by SULT2A1 and possibly other sulfotransferases.

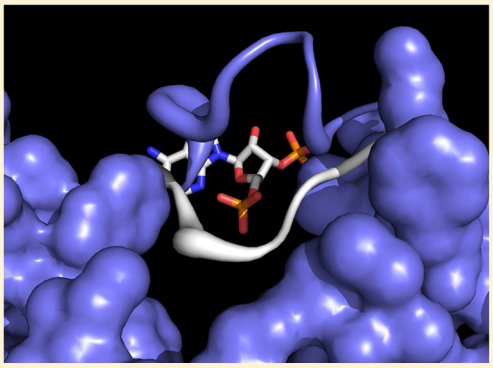

Sulfation of a biomolecule is often essential to controlling its biologic activity. Hundreds of molecules and their attendant metabolic processes are regulated via sulfation: steroid,[1−3] peptide,[4] dopamine,[5] and thyroid[6] receptors; the immune system;[7] lymph circulation;[8] hemostasis;[9] pheromone reception;[10] growth factor recognition;[11] etc. Normal functioning of these processes often depends on the presence or absence of a single, critically positioned sulfuryl group. Among the human diseases linked to improper sulfation are cancer of the breast[12] and endometrium,[13] Parkinson's disease,[14] cystic fibrosis,[15] hemophilia,[16] and heart disease.[1,17]

Transfer of the sulfuryl moiety ($-SO_3$) from activated sulfate [3′-phosphoadenosine 5′-phosphosulfate (PAPS)] to biological recipients is catalyzed by sulfotransferases.[18] Human cytosolic sulfotransferases are a small group (13 members) of conserved, soluble enzymes.[19] Four such sulfotransferases are detected in adult human liver.[20,21] In addition to their homeostatic functions,[2,22] these four enzymes sulfonate myriad compounds as they pass into the liver from the digestive tract.[18,23] Two of the enzymes, SULT1A1 and SULT2A1, comprise 80 − 90% of liver sulfotransferases by mass and are responsible for the majority of the sulfation that occurs there.[21] The specificities of these enzymes are necessarily broad, and together, they define the structures that are selected for sulfation from the liver milieu.[20,21] The molecular basis of this selection has not been defined and is the topic of this work.

SULT2A1 is known to sulfonate steroids, drugs, and other xenobiotics and is highly selective for DHEA (dehydroepiandrosterone).[18,24] DHEA, the most abundant circulating steroid in humans, is a pro-hormone that circulates in its sulfated form and can be converted, as needed, to any of a number of steroids in situ.[25] The sulfation of drugs is common and often prevents them from binding their receptors.[26] Raloxifene (Evista™), one of many drugs sulfated by SULT2A1, is taken daily by approximately 1.2 million women in the United States to prevent osteoporosis and decrease the risk of breast cancer.[27,28] The structures of raloxifene and DHEA differ markedly (Figure 1), yet both are believed to be efficiently sulfated by SULT2A1.[29,30] Raloxifene is composed of a planar steroid-like "base" structure whose dimensions are roughly similar those of DHEA and a large R group (the key to its receptor antagonism[31]) with dimensions also comparable those of

Received: May 15, 2012
Revised: June 15, 2012
Published: June 15, 2012

   dx.doi.org/10.1021/bi300631g | *Biochemistry* 2012, 51, 5674−5683

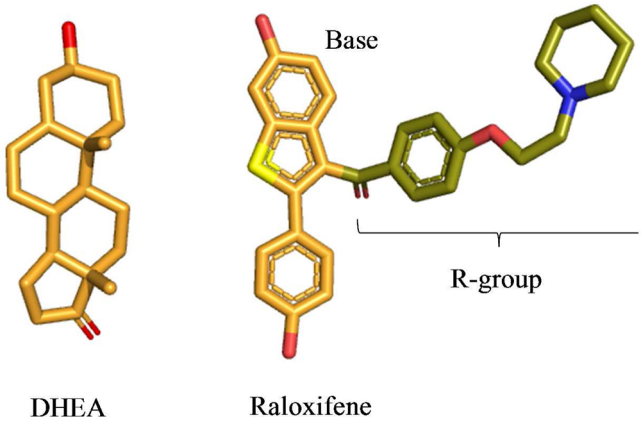

Figure 1. Structures of DHEA and raloxifene.

DHEA. Notably, DHEA is sulfated (>99%) in vivo,[32] and raloxifene is not.[33]

In an attempt to reconcile the in vivo and in vitro findings, we used raloxifene and DHEA as probes to explore the selectivity of SULT2A1. The study revealed that a previously undescribed 21-fold antisynergy between PAPS and raloxifene (but not DHEA) is the likely source of the discrepancy. Structures suggested the antisynergy might be due to a nucleotide-gated isomerization that causes an edge of the acceptor-binding pocket to "swing" into a position that sterically prevents access of raloxifene while admitting DHEA.[34−36] The model-specific predictions of the isomerization mechanism were tested in equilibrium and pre-steady-state ligand binding studies, and the results provide strong support for the mechanism. It appears that among the mechanisms used by sulfotransferases to select substrates is a PAPS-gated steric screen, a molecular sieve that rejects or accepts substrates on the basis of their dimensions.

MATERIALS AND METHODS

Dithiothreitol (DTT), EDTA, L-glutathione (reduced), glucose, imidazole, isopropyl thio-β-D-galactopyranoside (ITPG), LB13-member medium, lysozyme, β-mercaptoethanol, pepstatin A, raloxifene, DHEA, and potassium phosphate were of the highest grade available from Sigma. Ampicillin, HEPES, KOH, $MgCl_2$, NaCl, KCl, and phenylmethanesulfonyl fluoride were purchased from Fisher Scientific. [^{3}H]DHEA (90 Ci/mmol) was purchased from NEN Life Science Products, and [^{3}H]RAL (34.4 Ci/mmol) was purchased from Moravek Biochemical. Glutathione- and nickel-chelating resins were obtained from GE Healthcare. Competent *Escherichia coli* [BL21(DE3)] was purchased from Novagen. Simulations were performed on a Parallel Quantum Solution QS32-2670C-XS8 computer. MODELER was provided by the University of California (San Francisco, CA), and GOLD was obtained from the Cambridge Crystallographic Data Center.

Protein Purification. SULT2A1 DNA was inserted into a triple-tag pGEX-6P expression vector with an N-terminal His/GST/MBP tag.[22,37] The plasmid was transfected into BL21-(DE3) *E. coli* and was grown at 37 °C in LB medium containing ampicillin (100 g/mL) to an A_{600} of 0.7. Expression was induced with ITPG (0.7 mM). The temperature was reduced to 18 °C 8 h following induction, and cells were harvested 16 h later. SULT2A1 was purified according to a published protocol.[38] Briefly, the cell pellet was suspended in KPO_4 (50 mM, pH 7.3, 25 °C) containing lysozyme (0.10 mg/mL), PMSF (290 μM), pepstatin A (1.5 μM), KCl (0.40 M), and β-mercaptoethanol (5.0 mM). The mixture was stirred for 1 h at 4 °C prior to sonication (Branson Sonifier). Cell debris was removed by centrifugation (60 min, 4 °C, 34000*g*), and the supernatant was loaded onto a 5 mL Chelating Sepharose Fast Flow column charged with Ni^{2+}. The fusion protein was eluted from the Ni^{2+} column with imidazole (250 mM) directly onto a glutathione Sepharose column. The glutathione Sepharose column was then washed, and the fusion protein was eluted with GSH (10 mM). The fusion protein was then digested with Precision Protease via overnight dialysis against HEPES/K^+ (50 mM, pH 7.5), DTT (1.5 mM), and KCl (50 mM) at 4 °C. After dialysis, the sample was passed back through the glutathione column to remove the His/GST/MBP tag and Precision Protease. The flow-through containing SULT2A1 was collected and concentrated in an Amicon Ultra centrifugal filter (10 kDa cutoff) and stored at −80 °C in 40% glycerol. The protein preparations were assessed using sodium dodecyl sulfate−polyacrylamide gel electrophoresis and were >97% pure. Protein concentrations were determined spectrophotometrically (ε_{280} = 35.7 mM^{-1} cm^{-1}).[2]

Initial Rate Kinetics. Experimental design and solution compositions are described in the legend of Figure 2. Reactions were quenched by rapid hand mixing of 10 μL of the reaction mixture with 1.0 μL of 0.50 M KOH. Sulfated and nonsulfated acceptors were separated by extracting the nonsulfated species into choloroform using the following protocol: 190 μL of KPO_4 (25 mM, pH 8.8) was added to the quenched solution to neutralize the base and increase the volume, and 1.0 mL of chloroform was added and the mixture vortexed vigorously for 15 s and centrifuged. The aqueous phase was removed and again extracted with 1.0 mL of chloroform. The sulfated acceptor in the aqueous phase was quantified using a Perkin-Elmer W450624 scintillation spectrometer.

Ligand Binding Studies. *Binary Complexes.* Binding of the nucleotide and acceptor to SULT2A1 was monitored via changes in the intrinsic fluorescence of the enzyme at 290 nm (λ_{ex}) and 340 nm (λ_{em}). Titrants were added to a solution containing SULT2A1 (0.05 μM), $MgCl_2$ (5.0 mM), and KPO_4 (25 mM) at pH 7.4 and 25 ± 2 °C. Dilutions due to the addition of titrant were negligible (<1.8% at titration end points). Nucleotide was added from an aqueous buffered stock. Acceptor was added from a stock containing 50% ethanol. Controls ensured that the ethanol did not detectably contribute to fluorescence or modify the acceptor affinity. Titrations were performed in triplicate. The data were averaged and fit by least-squares fit to a model that assumes a single binding site per monomer.

Ternary Complex. Ternary complex interactions can cause K_d and fluorescence intensity to vary as the fixed variable ligand concentration is varied at subsaturating concentrations. To obtain K_d and amplitude intensities at saturation with both ligands, titrations were performed using a matrix of ligand concentrations and all curves were fit simultaneously using a global model. The concentration matrix consisted of 5 PAP and 12 donor concentrations. PAP ranged from 0 to 5K_d for the ternary complex; raloxifene and DHEA concentrations varied in equal increments from zero to 50 and 20 μM, respectively. Absolute PAP concentrations were as follows: 0, 5.0, 25, 50, and 125 μM PAP and 0, 1.0, 5.0, 10, and 25 μM PAP for the raloxifene and DHEA titrations. Conditions and protocols are described in the previous paragraph.

dx.doi.org/10.1021/bi300631g | *Biochemistry* 2012, 51, 5674−5683

Table 1. Initial Rate Kinetic Constants[a]

substrate	K_m (μM)	K_{ia} (μM)	K_{ia}/K_m	k_{cat} (s^{-1})	k_{cat}/K_m
DHEA	1.3 ± 0.1	1.8 ± 0.1	1.4 ± 0.2	0.7 ± 0.03	0.54 ± 0.07
PAPS	0.39 ± 0.01	0.47 ± 0.06			
RAL	24.8 ± 0.3	1.1 ± 0.1	23 ± 1.0	0.10 ± 0.01	0.004 ± 0.0003
PAPS	5.9 ± 0.6	0.24 ± 0.04			

[a]Estimates of the standard error are given.

Algebraic Model Used To Fit the Titration Data. The fluorescence intensity at a given ligand concentration (I_i) relative to that at zero ligand is given by eq 1:

$$\frac{I_i}{I_o} = \frac{\sum I_x E_x}{I_E E_T} \quad (1)$$

where E_x and I_x represent the concentration and concentration-normalized fluorescent intensity of each enzyme species. E_T is the total enzyme concentration. By substituting eq 2 into eq 1 and

$$E_T = E + EA + EB + EAB \quad (2)$$

using dissociation constants to express each species in terms of unliganded enzyme, I/I_o can be cast solely in terms of dissociation constants, ligand concentrations, and intensities. The result, eq 3, was used to fit the titrations.

$$\frac{I_i}{I_o} = \frac{c_1 K_{AB} + c_2 I_{AB}}{c_3 K_{AB} + c_4} \quad (3)$$

$$c_1 = I_E + I_{EA}\frac{A}{K_A} + I_{EB}\frac{B}{K_B} \quad (4)$$

where

$$c_2 = \frac{BA}{K_A} \quad (5)$$

$$c_3 = I_E\left(1 + \frac{A}{K_A} + \frac{B}{K_B}\right) \quad (6)$$

$$c_4 = I_E\frac{AB}{K_A} \quad (7)$$

I_i/I_o and parameters c_1–c_4 are known at each point in the ligand concentration matrix.

In Silico Docking of DHEA and RAL. A ligand-free model of SULT2A1 was constructed from the SULT2A1·DHEA [Protein Data Bank (PDB) entry 1J99][34] binary structure, and a model of the SULT2A1·PAPS structure was developed from the SULT2A1·PAP (PDB entry 1EFH)[35] binary structure. Each model was prepared using homology modeling with MODELER[39] to determine the position of missing atoms. A sulfuryl group was added to PAP to form PAPS in the SULT2A1·PAPS model. The models were then protonated and energy minimized using GOLD.[40] DHEA and RAL were docked into the models using a Lamarckian, evolution-based algorithm (GOLD). The lowest-energy orientation obtained after 2500 generations was analyzed and considered competent if the predicted free energy of binding was favorable and the ligand hydroxyl was properly oriented to accomplish catalysis and hydrogen bonded to H99, a universally conserved general base. Each simulation was repeated 10 times, and the lowest-energy structures were used in Figure 4.

Pre-Steady-State Binding. Pre-steady-state fluorescence experiments were performed using an Applied Photophysics SX20 stopped-flow spectrometer. Samples were excited at 285 nm, and light emitted above 320 nm was detected using a cutoff filter. The sequential mixing experiments were conducted with an SQ.1 sequential-mixing accessory. A solution containing SULT2A1 (0.10 μM), $MgCl_2$ (5.0 mM), and KPO_4 (25 mM, pH 7.4) at 25 ± 2 °C was rapidly mixed (1:1) with a solution lacking SULT2A1 but containing RAL, DHEA, or PAPS. Binding was monitored by following the changes in the intrinsic fluorescence of the enzyme. Typically, eight progress curves were collected at a given ligand concentration and averaged to produce a composite curve. Three independently acquired composite curves were averaged to generate the data set used to obtain apparent rate constants. Data were fit using Applied Photophysics Pro-Data analysis software (Marquardt fitting algorithm).

Fifteen percent of SULT2A1 denatures during the push phase of the stopped-flow experiment. Denaturation occurs before mixing in the optical cell and results in a slow decrease in fluorescence intensity caused by the settling of the precipitate. The rate and magnitude of the precipitation were remarkably consistent. The precipitation amplitude is small, and the settling rate is quite slow relative to those of ligand binding reactions ($k_{precipitate}$ = 0.030 s^{-1}). All binding data were corrected for precipitation during analysis.

RESULTS AND DISCUSSION

Raloxifene and PAPS Bind Antisynergistically. An initial rate study was performed to define differences in the interactions of raloxifene and DHEA with SULT2A1. The results indicate that raloxifene and DHEA behave similarly toward the unliganded enzyme but differ markedly in their interactions with E·PAPS (Table 1). The best-fit lines passing through the double-reciprocal plots of the data intersect below the horizontal axis when the acceptor is raloxifene and on (or near) the axis when it is DHEA (Figure 2A,B). The vertical component of this intersection is given by $k_{cat}(1 - K_m/K_i)$, where K_i and K_m represent the affinity of substrate A at concentrations of B extrapolated to zero and infinity, respectively. As such, the ratio of these constants reports the effect of B on the affinity of A and is a measure of substrate synergy. The kinetic constants reveal a 21-fold antisynergy in the interaction of PAPS and raloxifene and a slight positive synergy (1.4-fold) in the interactions with DHEA (Table 1). To the best of our knowledge, this is the first report of substrate antisynergism in the sulfotransferase field.

Raxofiene Is a Poor Substrate. Previous work suggests that the K_m for raloxifene is 3.5 μM.[29] This value was determined at a concentration of PAPS (10 μM) that far exceeds typical PAPS K_m values (~0.3 μM[30]) and was thought to be saturating. The current work, in which PAPS concentration is varied, reveals that the raloxifene K_m (25 μM) is considerably larger than originally thought. This

dx.doi.org/10.1021/bi300631g | Biochemistry 2012, 51, 5674–5683

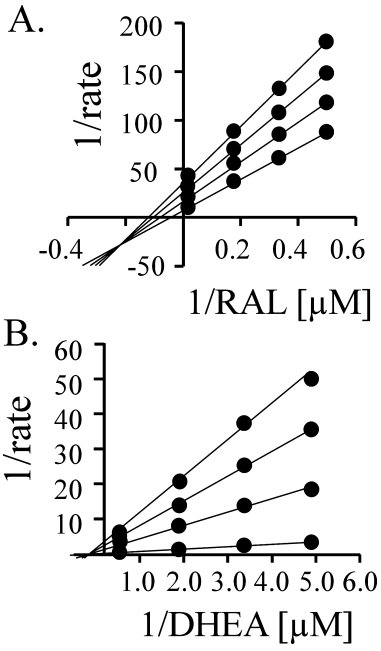

Figure 2. Initial rate study of raloxifene and DHEA sulfation. Rates were determined under each of the 16 conditions defined by a 4 × 4 matrix of substrate concentrations that varied from $0.2K_m$ to $5.0K_m$ in equal increments in double-reciprocal space. Reactions were initiated by the addition of PAPS to a solution containing the ^{3}H-labeled acceptor. Rates were obtained from slopes of four-point progress curves in which <5% of the concentration-limiting reactant consumed at the reaction end point was converted to product. Conditions were as follows: SULT2A1 (0.20 μM), $MgCl_2$ (5.0 mM), KPO_4 (25 mM, pH 7.4), 25 ± 2 °C. Raloxifene and DHEA concentrations are indicated in the figures. PAPS concentrations were as follows: (A) 30, 3.3, 1.8, and 1.2 μM and (B) 2.5, 0.28, 0.15, and 0.1 μM. Each point represents the average of two independent determinations. The lines through the points represent behavior predicted by a weighted least-squares fit to a sequential bi-bi model.[48] Quenching, separation, and quantitation protocols are described in Materials and Methods.

difference is due to the subsaturating concentration of PAPS used in the earlier study ($1.7K_m$). The kinetic constants in Table 1 predict an apparent K_m for raloxifene at 10 μM PAPS of 5.1 μM, which agrees reasonably with the earlier work. k_{cat}/K_m, the second-order rate constant for conversion of substrate to product, is often taken as a measure of the selectivity of an enzyme toward a particular substrate. k_{cat}/K_m for DHEA is 135-fold greater than that for raloxifene; thus, at identical concentrations of DHEA and raloxifene (where $[S] \ll K_m$ for both substrates), DHEA will be sulfated 135-fold faster than raloxifene. Relative to DHEA, raloxifene is a poor substrate, and it is perhaps not surprising that it is not sulfated well in vivo.[33]

Ligand Binding at Equilibrium. The initial rate studies reveal antisynergistic interactions between raloxifene and PAPS, but not DHEA. If the binding reactions are at or near equilibrium during turnover, the differences in interaction are due to changes either in the ligand binding equilibrium constants or in equilibria linked to the binding reaction. If binding is not at equilibrium, because of turnover, the differences are due to the changes in the steady-state "set points" of the binding reactions that occur when raloxifene is "swapped" for DHEA. Shifting away from equilibrium typically causes steady-state affinity constants to be larger than their analogous equilibrium values. Equilibrium effects are caused by the shifting of Gibbs potentials of stable enzyme forms relative to one another, whereas steady-state effects are due to changes in relative magnitudes of rate constants that govern separate steps in the mechanism. Thus, distinguishing equilibrium from steady-state mechanisms is tantamount to determining whether antisynergy is due to changes in ground- or transition-state energetics.

The equilibrium binding interactions between the nucleotide and acceptor were studied via fluorescence titrations (Figure 3). SULT2A1 undergoes substantial decreases (20−60%) in

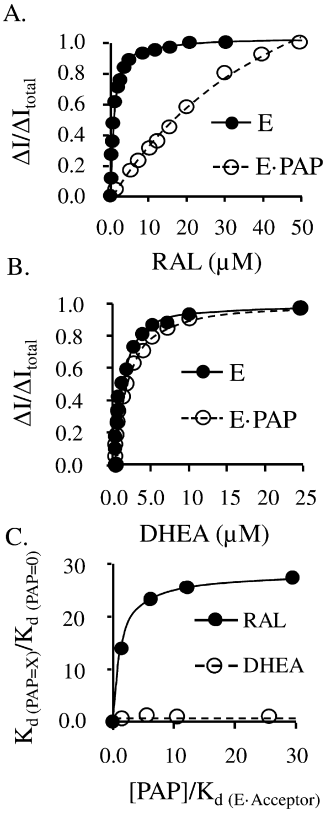

Figure 3. Equilibrium binding of RAL and DHEA to SULT2A1. (A) Raloxifene binding to E and E·PAP. Binding is monitored by changes in the intrinsic enzyme fluorescence (λ_{ex} = 290 nm, and λ_{em} = 340 nm). The solution consisted of SULT2A1 (0.20 μM), PAP (0 or 125 μM), $MgCl_2$ (5.0 mM), and KPO_4 (25 mM, pH 7.4) at 25 ± 2 °C. The fluorescence intensity (ΔI) is normalized to the total fluorescence change (ΔI_{total}). Each point is the average of two independent determinations. The line through the data is the behavior predicted by least-squares fitting using a model that assumes a single binding site per subunit. Further details are described in Materials and Methods. (B) DHEA binding to E and E·PAP. Conditions were identical to those described for panel A except that the PAP concentration was 25 μM. (C) Quantitating ternary complex binding interactions. Raloxifene solubility prevents saturation of the ternary complex. To quantitate the ternary complex interactions, titrations with the acceptor were conducted at series of five PAP concentrations, and K_d values were obtained by simultaneously fitting the data from the five titrations. *Y*-axis values report fold change in the acceptor affinity constant and are given as the ratio of K_d at a fixed non-zero PAP concentration to that at zero PAP $[K_{d(PAP=X)}/K_{d(PAP=0)}]$. PAP concentrations were selected to range from 0 to 25 times its ternary complex K_d; hence, *X*-axis values are given as the PAP concentration divided by its affinity constant $[[PAP]/K_{d(E\cdot acceptor)}]$. The absolute PAP concentrations were 0, 5.0, 25, 50, and 125 μM (raloxifene titration) and 0, 1.0, 5.0, 10, and 25 μM (DHEA titration). Further details are given in Materials and Methods.

dx.doi.org/10.1021/bi300631g | *Biochemistry* 2012, 51, 5674−5683

intrinsic fluorescence (λ_{ex} = 290 nm, and λ_{em} = 340 nm) in response to the formation of binary or ternary complexes. PAP, rather than PAPS, was used in these studies to avoid complications caused by turnover. The binding constants obtained from the titrations agree well with the analogous initial rate constants, suggesting that PAP is a reasonable surrogate for PAPS. Further support for this position is given by the results of the pre-steady-state binding experiments described below. These experiments utilize PAPS and circumvent the turnover issue by monitoring binding on time scales that are short relative to that of turnover. The affinities obtained in the pre-steady-state work are nearly identical to the equilibrium binding affinities determined using PAP.

The results of the binding studies are presented in Figure 3 and Table 2. The data are plotted as the fraction change in fluorescence ($\Delta I/\Delta I_{tot}$) versus concentration. PAP and PAPS bind E with virtually identical affinities, 280 and 300 nM, respectively (Table 2); hence, addition of the moiety that is transferred during chemistry contributes little to binding affinity. The binding of raloxifene and DHEA to E and E·PAP is shown in panels A and B of Figure 3, respectively. The PAP concentration in these titrations, 125 μM, is sufficiently high that the enzyme remains saturated with nucleotide throughout the four titrations shown in panels A and B. Having PAP bound clearly weakens the affinity of raloxifene and has no discernible effect on the affinity of DHEA. The solubility of raloxifene (K_s = 55 μM [27]) is sufficiently high to allow saturation of E (K_d = 1.1 μM) but not E·PAPS (K_d = 25 μM). The highest raloxifene concentration used in the panel A titration (50 μM) is near the limit of its solubility. Saturation with raloxifene was not achieved in this titration; consequently, reliable binding constants and amplitudes could not be obtained. Had saturation occurred, the associated binding constant and amplitude would pertain to only a single PAPS concentration. These problems were solved by performing acceptor titrations at a series of five PAP concentrations and fitting the titrations simultaneously to extract true ternary complex amplitudes and affinity constants (Materials and Methods). The result of the fit is presented in Figure 3C. The *Y*-axis is given in terms of fold antisynergy, that is, K_d at a given PAP concentration to that at zero PAP. The PAP concentrations in these titrations ranged from 0 to 25 times the ternary complex K_d; thus, the *X*-axis is given as [PAP]/$K_{d\ ternary}$. The plot demonstrates a pronounced, saturable binding antisynergy between PAP and raloxifene, and virtually no interaction between PAP and DHEA (synergy estimated to be 1.1 ± 0.2). The fit predicts a 21-fold antisynergy (1.8 kcal/mol), which agrees well with the initial rate value (23-fold or 2.0 kcal/mol). The close agreement of the equilibrium binding and initial rate affinity constants for all ligands and complexes argues that the ligand interactions during turnover are due primarily to ground-state interactions and that ligand binding is near equilibrium during turnover.

Table 2. Equilibrium Binding Constants

ligand	enzyme species[a]	K_d (μM)[b]
PAP	E·	0.30 ± 0.04
PAPS	E·	0.28 ± 0.03
DHEA	E·	1.0 ± 0.08
Ral	E·	1.1 ± 0.2
PAP	DHEA·E·	0.21 ± 0.05
PAP	Ral·E·	6.0 ± 0.7
DHEA	PAP·E·	1.1 ± 0.2
Ral	PAP·E·	29 ± 4

[a]Dots denote unoccupied binding sites. [b]Estimates of the standard error are given.

Kinetic Mechanism of SULT2A1. The kinetic mechanism of SULT2A1 has not been determined; however, the mechanisms of other SULTS have been studied and are described as either ordered- or random-sequential.[2,41] The initial rate pattern presented in Figure 2 is consistent with steady-state ordered or random mechanisms and a random mechanism in which substrate binding is near equilibrium during turnover. The data argue against an ordered mechanism in which binding of the first substrate is at equilibrium, which predicts double-reciprocal data that intersect on the vertical axis.[42] The close agreement between the equilibrium binding and initial rate constants for all binary and ternary complexes strongly suggests that the binding reactions are near equilibrium during turnover. The results are not easily reconciled with a steady-state ordered mechanism. For example, the second substrate to add in the ordered mechanism would have to bind the enzyme nonproductively in the absence of the first. Such binding typically results in substrate inhibition with K_i equal to K_d, which is not observed. Further, the mechanism's rate constants would have to balance such that each of the steady-state affinity constants happened to equal their corresponding equilibrium binding constants (including the nonproductive binding constants) for both the raloxifene and DHEA reactions, an unlikely scenario. In summary, the data provide strong support for only the rapid-equilibrium random mechanism.

A Molecular Model of Antisynergy. Crystal structures of SULT2A1 binary complexes offer a molecular explanation for the different response of the enzyme to DHEA and raloxifene. SULT2A1 harbors a 23-reside, conserved active site "lid" (N226−D253) that restructures differently upon binding of the donor or acceptor. SULT2A1 is the only sulfotransferase for which structures of both donor (PDB entry 1EFH) and acceptor binary complexes (PDB entry 1J99) are available.[34,35,43,44] The acceptor complexes show an open lid that accommodates binding of either DHEA or raloxifene, and both ligands dock well into the open structure in silico (Materials and Methods). A nine-residue segment of the lid (N230−Y238) situated at the entrance of the acceptor binding pocket is repositioned upon PAPS binding, with the result that the entrance is constricted to point that it will admit only DHEA; this too is supported by in silico docking. Thus, the nine-residue segment appears to function as a molecular gate that restricts access to the acceptor site when "driven" into position by the binding of a nucleotide. The open and closed positions of the gate are colored white and blue, respectively, in Figure 4. DHEA appears to be capable of forming a reactive complex with either form of the enzyme (panel A), whereas raloxifene can access only the open form because of steric hindrance from the PAP-stabilized, closed gate (panel B).

Predictions of the Gate Model. The gate model predicts that substrates too large pass through the closed pore cannot bind to the enzyme, yet initial rate and equilibrium binding measurements clearly demonstrate that raloxifene binds to the nucleotide-closed enzyme. The binding and structural data are reconciled if the enzyme is allowed to oscillate between open and closed forms when the nucleotide is bound. In this case, the affinity of the large substrate will appear to decrease by a factor

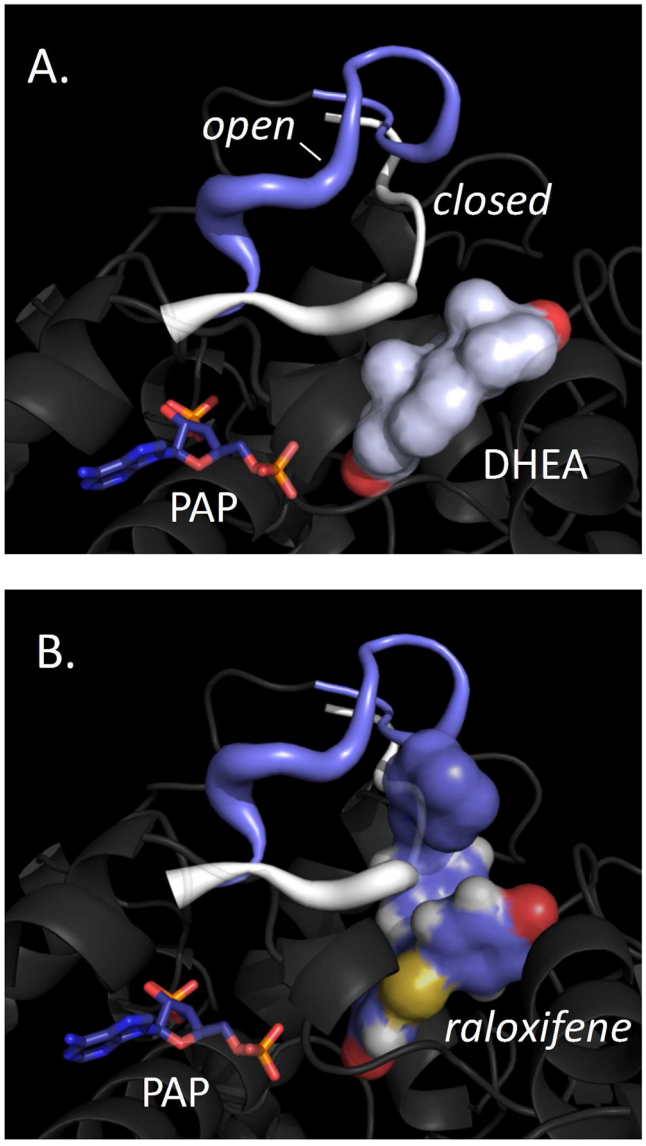

Figure 4. Nucleotide-linked gate closure discriminates substrates. (A) DHEA is positioned well for chemistry in the open and closed complexes. (B) Raloxifene is sterically prevented from accessing the acceptor binding pocked in the closed but not the open complex. Open and closed models were constructed from the SULT2A1·DHEA (PDB entry 1J99) and SULT2A1·PAP (PDB entry 1EFH) binary structures, and ligands were docked using an evolution-based algorithm (Materials and Methods).

that corresponds to the fold decrease in the concentration of the nucleotide-bound open form, which is given by the equilibrium constant for the isomerization between the open and closed states. This mechanism also predicts that the apparent change in affinity will be due exclusively to a change in the on-rate constant, because the origin of the effect is a simple decrease in the concentration of the open form. If, on the other hand, an isomerization is not operative, the closed form seen in the crystal is not representative of the enzyme in solution, and antisynergy must be due to allosteric interactions that alter the form of the enzyme to which the acceptor binds. In such cases, changes in affinity can be caused by changes in on- and/or off-rate constants. Importantly, microscopic reversibility requires that allosteric interactions have identical energetic consequences for either ligand during binding; consequently, effects on the PAPS and raloxifene on- and off-rate constants should be identical. In contrast, a mechanism in which isomerization simply decreases the concentration of the acceptor binding form of the enzyme makes no such prediction.

Testing the Predictions. To test the gate model, on- and off-rate constants for the binding of raloxifene to E and E·PAPS were determined. Binding was monitored via changes in the intrinsic fluorescence of SULT2A1. Reactions were initiated by rapidly mixing a solution containing PAPS (200 μM) and SULT2A1 (0.20 μM) with an equal volume of a solution containing a fixed-variable concentration of raloxifene (Figure 5A,B). The PAPS concentration after mixing was sufficiently

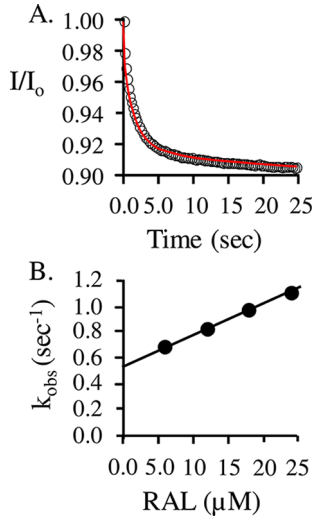

Figure 5. Pre-steady-state binding of RAL to SULT2A1. (A) Binding of raloxifene to E. Binding reactions were initiated by rapidly (1:1) mixing a solution containing RAL (2.0 μM) with a solution containing SULT2A1 (0.10 μM). Binding was monitored by changes in the intrinsic enzyme fluorescence (λ_{ex} = 290 nm, and $\lambda_{em} \geq$ 330 nm). Fluorescence changes are given relative to the intensity (I/I_o) at time zero. Each point represents the average of three independent determinations. The curve through the data represents the behavior predicted by the best fit to a single-exponential model. The solution consisted of $MgCl_2$ (5.0 mM) and KPO_4 (25 mM, pH 7.4) at 25 ± 2 °C. (B) k_{obs} vs raloxifene concentration. Progress curves were obtained at four concentrations of raloxifene, and conditions are given in the legend for panel A. Reactions were pseudo-first-order in raloxifene in all cases, and apparent rate constants were obtained by fitting with a single-exponential model. Similar studies were performed for the binding of DHEA and raloxifene to E and E·PAP. Results are compiled in Table 3.

high to saturate the ternary complex ($23K_m$), and controls ensured that <1.0% of the E·PAPS complex was hydrolyzed to E·PAP during the experiments. Conditions were such that <2% of the total raloxifene was enzyme-bound at the reaction end point in all cases; hence, the reactions could be treated as pseudo-first-order reactions and fit using a single-exponential equation. The apparent rate constants obtained from the fits were plotted versus raloxifene concentration, and the resulting plot was fit to a linear equation to obtain k_{on} and k_{off}[45] (Figure 5B).

The results of the pre-steady-state binding studies are precisely those predicted by the isomerization mechanism; the effects of PAPS on raloxifene binding are virtually entirely due to changes in the on-rate constant (Table 3). The raloxifene on-rate constant decreases 19-fold when PAPS is

dx.doi.org/10.1021/bi300631g | Biochemistry 2012, 51, 5674−5683

Table 3. Acceptor Binding Rate Constants[a]

ligand	enzyme species[b]	k_{on} (M^{-1} s^{-1})	k_{off} (s^{-1})	K_d (μM) (k_{off}/k_{on})
DHEA	E·	(2.0 ± 0.2) × 10^6	2.1 ± 0.1	1.1 ± 0.1
DHEA	PAPS·E·	(2.1 ± 0.1) × 10^6	3.0 ± 0.1	1.1 ± 0.1
Ral	E·	(4.1 ± 0.1) × 10^5	0.47 ± 0.03	1.4 ± 0.1
Ral	PAPS·E·	(2.2 ± 0.3) × 10^4	0.54 ± 0.03	25 ± 5

[a]Estimates of the standard error are given. [b]Dots denote unoccupied binding sites.

bound, while the rate constants for dissociation from raloxifene·E and raloxifene·E·PAPS are nearly identical. It should be noted that the dissociation constants for the binding of raloxifene to E and E·PAPS calculated from the rate constants (1.1 and 25 μM, respectively) agree well with the analogous initial rate constants (1.1 and 23 μM, respectively), further confirming that ligand binding is near equilibrium during turnover.

The Gate Is Noninteractive. The initial rate and equilibrium binding measurements reveal that nucleotide has little if any influence on the affinity of DHEA but do not rule out the possibility that the DHEA binding on- and off-rate constants are affected equally by the nucleotide. If so, the gate interacts with DHEA during ingress and egress and may have selective properties beyond "simple" sieving. If, on the other hand, closing the gate does not influence the rate constants, it functions as a noninteractive molecular sieve that admits or prevents ligands on the basis of geometry. The data clearly show that DHEA binding rate constants are not influenced significantly by the presence of PAPS (Table 4).

Table 4. PAPS Binding Rate Constants[a]

ligand	enzyme species[b]	k_{on} (M^{-1} s^{-1})	k_{off} (s^{-1})	K_d (μM) (k_{off}/k_{on})
PAPS	E·	(8.6 ± 0.5) × 10^6	2.3 ± 0.3	0.27 ± 0.06
PAPS	DHEA·E·	(7.9 ± 0.4) × 10^6	1.9 ± 0.2	0.24 ± 0.09
PAPS	RAL·E·	(8.3 ± 0.36) × 10^6	50 ± 2	6.0 ± 0.6

[a]Estimates of the standard error are given. [b]Dots denote unoccupied binding sites.

PAPS Binding. Structures predict that raloxifene prevents the gate from closing (Figure 4). Consequently, the molecular circuitry that links PAPS binding to gate closure cannot be established, resulting in a 21-fold decrease in PAPS affinity. Weakened binding can be caused by changes in on- or off-rate constants. A decrease in the on-rate constant reflects stabilization of structural features that inhibit binding, while an increased off-rate constant requires a weakening of the factors that prevent release. To better understand how different enzyme forms respond to nucleotide, the microscopic rate constants for the binding of PAPS to E, E·DHEA, and E·raloxifene were determined and compared.

Stopped-flow fluorescence was used to obtain PAPS binding rate constants. Experimental protocols are detailed in Materials and Methods and closely resemble those used in the pre-steady-state binding experiments described above. Briefly, reactions were pseudo-first-order in ligand, and progress curves were fit using a single-exponential model to obtain the apparent rate constants needed to determine k_{on} and k_{off}. Binding of PAPS to E·DHEA was studied under conditions where enzyme remained saturated with DHEA throughout the binding reactions. Saturation of the ternary complex with raloxifene is not possible because of its limited solubility (K_s = 55 μM[27]). Reactions involving raloxifene were initiated by mixing equal volumes of a solution containing PAPS (100–250 μM) and raloxifene (50 μM) with a solution containing SULT2A1 (50 nM) and raloxifene (50 μM). At 50 μM, raloxifene saturates E ($50K_d$) but not the ternary complex ($\sim 2K_d$). Thus, prior to being mixed with PAPS, the enzyme is saturated with raloxifene. After mixing, raloxifene dissociates as the ternary complex forms, leading to an increase in fluoresence. The rate at which PAPS binds depends linearly on is concentration, while raloxifene dissociation is independent of PAPS concentration. Given the relatively slow rate at which raloxifene dissociates from the ternary complex (k_{off} = 0.54 s^{-1}), it was possible to increase the PAPS concentration and cleanly separate the PAPS binding and DHEA dissociation phases. A PAPS concentration-optimized progress curve is shown in Figure 6A. The two phases are clearly identifiable, and the line

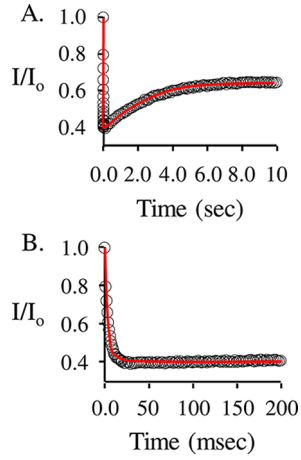

Figure 6. Pre-steady-state binding of PAPS to SULT2A1·raloxifene. (A) Progress curve for the binding of PAPS to E·raloxifene. A solution containing PAPS (100 μM) and raloxifene (50 μM) was mixed rapidly (1:1) with a solution containing SULT2A1 (0.05 μM) and raloxifene (50 μM). The raloxifene concentration (50 μM) is saturating with respect to the binary complex ($45K_d$) and subsaturating with respect to the ternary complex ($2.0K_d$). The addition of PAPS forms a ternary complex (causing the early phase decrease in the magnitude of the signal) and initiates dissociation of raloxifene (causing the subsequent increase). PAPS concentrations were sufficiently high to be pseudo-first-order and to achieve good separation of the phases. The conditions consisted of $MgCl_2$ (5.0 mM), KPO_4 (25 mM, pH 7.4), and 25 ± 2 °C. Fluorescence was excited at 290 nm and detected above 330 nm using a cutoff filter. Each point represents the average of three independent determinations. The curve through the data is the behavior predicted by the best fit obtained using a double-exponential model (see Materials and Methods). (B) Expanded view of panel A. The time axis of the data in panel A is expanded to highlight the separation of PAPS binding and raloxifene dissociation reactions. The PAPS concentration of 100 μM used in this experiment was the lowest concentration used in constructing the k_{obs} vs PAPS concentration plot from which rate constants were obtained (Table 4).

through the data is the behavior predicted by a double-exponential fit. Panel B expands the time axis of the data in the vicinity of the first phase to emphasize the separation. As expected, the rate constants associated with the first phase depend linearly on PAPS concentration and were used to obtain k_{on} and k_{off}, and the second-phase rate constant (0.51 ± 0.05 s^{-1}) is independent of PAPS concentration and similar to the raloxifene ternary complex k_{off}, 0.54 s^{-1}.

dx.doi.org/10.1021/bi300631g | Biochemistry 2012, 51, 5674–5683

The results of the PAPS binding studies are compiled in Table 4. Remarkably, the on-rate constants for binding of PAPS to E, E·DHEA, and E·raloxifene are identical within error, indicating that the energetic and presumably structural landscape experienced by PAPS as it binds to the enzyme is independent of ligand. Given that raloxifene prevents closure and DHEA does not, the identical on-rate constants suggest that binding and closure are separable. The off-rate constants for dissociation of PAPS from PAPS·E and PAPS·E·DHEA are also identical within error (2.1 s^{-1}); however, the escape of PAPS from the PAPS·E·raloxifene complex is 24-fold faster (50 s^{-1}). In the closed enzyme, the nucleotide is encapsulated by its binding pocket such that it can neither add to nor escape from the enzyme (Figure 7). Here again, the structure makes a testable prediction. If the nucleotide escapes only from the open form, the isomerization equilibrium constant predicts that it will do so 21-fold more slowly from complexes that can close (PAPS·E and PAPS·E·DHEA) than from those that cannot (PAPS·E·raloxifene), which is precisely what is observed.

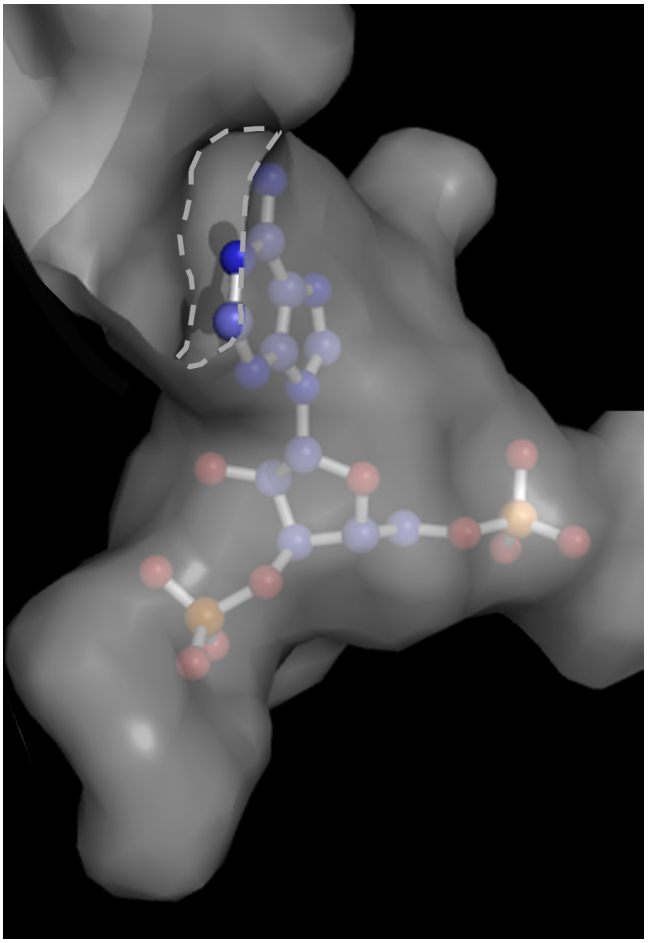

Figure 7. Closed structure that encapsulates PAPS. The active site surface of the closed form of SULT2A1 is shown "wrapped" around the nucleotide. The limited access of the nucleotide to solvent is highlighted by the dashed line circumscribing the only accessible solvent interface. Structural change is required to release the nucleotide.

In summary, "cap" closure is capable of encapsulating both substrates but is allosterically linked only to the binding of the nucleotide. Closure occurs in at least two, separable steps (nucleotide binding and cap restructuring), and it is possible to trap the enzyme in an open complex in which the nucleotide has bound but cannot form the stabilizing linkages that couple binding to closure. Conversely, the binding of a large acceptor disrupts the allosteric linkages, opening the PAPS-binding pocket and allowing the nucleotide to escape. Notably, PAPS concentrations in human tissue are reported to range from 10 to 80 μM.[46,47] Thus, in its native milieu, the enzyme is expected to be nucleotide-bound regardless of the acceptor and the selectivity of the closed gate will be maximally expressed.

■ CONCLUSIONS

The equivalence of initial rate and equilibrium binding constants of SULT2A1 substrates establishes that binding is random and near equilibrium during turnover and that substrates are selected, in significant measure, on the basis of antisynergy in ground-state binding interactions. Structures suggest that this selection is rooted in a nucleotide-driven restructuring of the acceptor-binding pocket that results in partial closure of an active site pore that sieves substrates on the basis of their dimensions. Reconciling the structural model with the binding data requires the nucleotide-bound form of the enzyme to isomerize between open and closed states, and that acceptors too large to pass through the pore will bind only the open form, while those small enough will bind both. This mechanism predicts that the concentration of the open form will be reduced when the nucleotide is bound by a factor given by the isomerization equilibrium constant. Consequently, the high substrate affinity constants will appear to decrease by the same factor despite the fact that the affinity for the open form has not changed. A further consequence of the reduced concentration is that the effects on binding will appear to be due exclusively to changes in the on-rate constant, and the binding and on-rate constant effects will be equivalent. These predictions are well supported by the experimental results and suggest that this molecular sieving mechanism is germane to SULT2A1 substrate selection and possibly that of other cytosolic sulfotransferases.

■ AUTHOR INFORMATION

Corresponding Author

*Department of Microbiology and Immunology, Albert Einstein College of Medicine, 1300 Morris Park Ave., Bronx, NY 10461-1926. Phone: (718) 430-2857. Fax: (718) 430-8711. E-mail: leyh@einstein.yu.edu.

Funding

Supported by National Institutes of Health Grants GM389532 and GM54469.

Notes

The authors declare no competing financial interest.

■ ABBREVIATIONS

DHEA, 5-dehydroepiandrosterone; DTT, dithiothreitol; EDTA, ethylenediaminetetraacetic acid; GSH, glutathione; GST, glutathione *S*-transferase; HEPES, *N*-(2-hydroxyethyl)-piperazine-*N*′-2-ethanesulfonic acid; IPTG, isopropyl β-D-1-thiogalactopyranoside; LB, Luria broth; MBP, maltose binding protein; PAP, 3′,5′-diphosphoadenosine; PAPS, 3′-phosphoadenosine 5′-phosphosulfate; PMSF, phenylmethanesulfonyl fluoride; raloxifene, [6-hydroxy-2-(4-hydroxyphenyl)-benzothiophen-3-yl]{4-[2-(1-piperidyl)ethoxy]phenyl}-methanone; SULT, cytosolic sulfotransferase.

REFERENCES

(1) Bai, Q., Xu, L., Kakiyama, G., Runge-Morris, M. A., Hylemon, P. B., Yin, L., Pandak, W. M., and Ren, S. (2011) Sulfation of 25-hydroxycholesterol by SULT2B1b decreases cellular lipids via the LXR/SREBP-1c signaling pathway in human aortic endothelial cells. *Atherosclerosis 214*, 350−356.

(2) Zhang, H., Varlamova, O., Vargas, F. M., Falany, C. N., and Leyh, T. S. (1998) Sulfuryl transfer: The catalytic mechanism of human estrogen sulfotransferase. *J. Biol. Chem. 273*, 10888−10892.

(3) Parker, C. R. (1999) Dehydroepiandrosterone and dehydroepiandrosterone sulfate production in the human adrenal during development and aging. *Steroids 64*, 640−647.

(4) Matsubayashi, Y., and Sakagami, Y. (2006) Peptide hormones in plants. *Annu. Rev. Plant Biol. 57*, 649−674.

(5) Goldstein, D. S., Swoboda, K. J., Miles, J. M., Coppack, S. W., Aneman, A., Holmes, C., Lamensdorf, I., and Eisenhofer, G. (1999) Sources and physiological significance of plasma dopamine sulfate. *J. Clin. Endocrinol. Metab. 84*, 2523−2531.

(6) Visser, T. J. (1994) Role of sulfation in thyroid hormone metabolism. *Chem.-Biol. Interact. 92*, 293−303.

(7) Selvan, R. S., Ihrcke, N. S., and Platt, J. L. (1996) Heparan sulfate in immune responses. *Ann. N.Y. Acad. Sci. 797*, 127−139.

(8) Tangemann, K., Bistrup, A., Hemmerich, S., and Rosen, S. D. (1999) Sulfation of a high endothelial venule-expressed ligand for L-selectin. Effects on tethering and rolling of lymphocytes. *J. Exp. Med. 190*, 935−942.

(9) Anderson, J. A., Fredenburgh, J. C., Stafford, A. R., Guo, Y. S., Hirsh, J., Ghazarossian, V., and Weitz, J. I. (2001) Hypersulfated low molecular weight heparin with reduced affinity for antithrombin acts as an anticoagulant by inhibiting intrinsic tenase and prothrombinase. *J. Biol. Chem. 276*, 9755−9761.

(10) Stowers, L., and Logan, D. W. (2010) Sexual dimorphism in olfactory signaling. *Curr. Opin. Neurobiol. 20*, 770−775.

(11) Mesiano, S., and Jaffe, R. B. (1997) Developmental and functional biology of the primate fetal adrenal cortex. *Endocr. Rev. 18*, 378−403.

(12) Falany, J. L., Macrina, N., and Falany, C. N. (2002) Regulation of MCF-7 breast cancer cell growth by β-estradiol sulfation. *Breast Cancer Res. Treat. 74*, 167−176.

(13) Falany, J. L., and Falany, C. N. (1996) Regulation of estrogen sulfotransferase in human endometrial adenocarcinoma cells by progesterone. *Endocrinology 137*, 1395−1401.

(14) Steventon, G. B., Heafield, M. T., Waring, R. H., and Williams, A. C. (1989) Xenobiotic metabolism in Parkinson's disease. *Neurology 39*, 883−887.

(15) Li, L., and Falany, C. N. (2007) Elevated hepatic SULT1E1 activity in mouse models of cystic fibrosis alters the regulation of estrogen responsive proteins. *J. Cystic Fibrosis 6*, 23−30.

(16) Moore, K. L. (2003) The biology and enzymology of protein tyrosine O-sulfation. *J. Biol. Chem. 278*, 24243−24246.

(17) Kase, E. T., Andersen, B., Nebb, H. I., Rustan, A. C., and Thoresen, G. H. (2006) 22-Hydroxycholesterols regulate lipid metabolism differently than T0901317 in human myotubes. *Biochim. Biophys. Acta 1761*, 1515−1522.

(18) Falany, C. N. (1997) Enzymology of human cytosolic sulfotransferases. *FASEB J. 11*, 206−216.

(19) Blanchard, R. L., Freimuth, R. R., Buck, J., Weinshilboum, R. M., and Coughtrie, M. W. (2004) A proposed nomenclature system for the cytosolic sulfotransferase (SULT) superfamily. *Pharmacogenetics 14*, 199−211.

(20) Teubner, W., Meinl, W., Florian, S., Kretzschmar, M., and Glatt, H. (2007) Identification and localization of soluble sulfotransferases in the human gastrointestinal tract. *Biochem. J. 404*, 207−215.

(21) Riches, Z., Stanley, E. L., Bloomer, J. C., and Coughtrie, M. W. (2009) Quantitative evaluation of the expression and activity of five major sulfotransferases (SULTs) in human tissues: The SULT "pie". *Drug Metab. Dispos. 37*, 2255−2261.

(22) Comer, K. A., Falany, J. L., and Falany, C. N. (1993) Cloning and expression of human liver dehydroepiandrosterone sulphotransferase. *Biochem. J. 289* (Part 1), 233−240.

(23) Dong, D., Ako, R., and Wu, B. (2012) Crystal structures of human sulfotransferases: Insights into the mechanisms of action and substrate selectivity. *Expert Opin. Drug Metab. Toxicol. 8*, 635−646.

(24) Falany, C. N., Wheeler, J., Oh, T. S., and Falany, J. L. (1994) Steroid sulfation by expressed human cytosolic sulfotransferases. *J. Steroid Biochem. Mol. Biol. 48*, 369−375.

(25) Labrie, F. (1991) Intracrinology. *Mol. Cell. Endocrinol. 78*, C113−C118.

(26) Lindsay, J., Wang, L. L., Li, Y., and Zhou, S. F. (2008) Structure, function and polymorphism of human cytosolic sulfotransferases. *Curr. Drug Metab. 9*, 99−105.

(27) Snyder, K. R., Sparano, N., and Malinowski, J. M. (2000) Raloxifene hydrochloride. *Am. J. Health-Syst. Pharm. 57*, 1669−1675 (quiz 1676−1668).

(28) Jordan, V. C. (2007) SERMs: Meeting the promise of multifunctional medicines. *J. Natl. Cancer Inst. 99*, 350−356.

(29) Falany, J. L., Pilloff, D. E., Leyh, T. S., and Falany, C. N. (2006) Sulfation of raloxifene and 4-hydroxytamoxifen by human cytosolic sulfotransferases. *Drug Metab. Dispos. 34*, 361−368.

(30) Falany, C. N., Vazquez, M. E., and Kalb, J. M. (1989) Purification and characterization of human liver dehydroepiandrosterone sulphotransferase. *Biochem. J. 260*, 641−646.

(31) Brzozowski, A. M., Pike, A. C., Dauter, Z., Hubbard, R. E., Bonn, T., Engstrom, O., Ohman, L., Greene, G. L., Gustafsson, J. A., and Carlquist, M. (1997) Molecular basis of agonism and antagonism in the oestrogen receptor. *Nature 389*, 753−758.

(32) Heroux, J. A., Falany, C. N., and Roth, J. A. (1989) Immunological characterization of human phenol sulfotransferase. *Mol. Pharmacol. 36*, 29−33.

(33) Cubitt, H. E., Houston, J. B., and Galetin, A. (2011) Prediction of human drug clearance by multiple metabolic pathways: Integration of hepatic and intestinal microsomal and cytosolic data. *Drug Metab. Dispos. 39*, 864−873.

(34) Rehse, P. H., Zhou, M., and Lin, S. X. (2002) Crystal structure of human dehydroepiandrosterone sulphotransferase in complex with substrate. *Biochem. J. 364*, 165−171.

(35) Pedersen, L. C., Petrotchenko, E. V., and Negishi, M. (2000) Crystal structure of SULT2A3, human hydroxysteroid sulfotransferase. *FEBS Lett. 475*, 61−64.

(36) Cook, I. T., Leyh, T. S., Kadlubar, S. A., and Falany, C. N. (2010) Structural Rearrangment of SULT2A1: Effects on dehydroepiandrosterone and raloxifene sulfation. *Horm. Mol. Biol. Clin. Invest. 1*, 81−87.

(37) Sun, M., and Leyh, T. S. (2010) The human estrogen sulfotransferase: A half-site reactive enzyme. *Biochemistry 49*, 4779−4785.

(38) Andreassi, J. L., and Leyh, T. S. (2004) Molecular functions of conserved aspects of the GHMP kinase family. *Biochemistry 43*, 14594−14601.

(39) Eswar, N., Webb, B., Marti-Renom, M. A., Madhusudhan, M. S., Eramian, D., Shen, M. Y., Pieper, U., and Sali, A. (2006) Comparative protein structure modeling using Modeller. *Current Protocols in Bioinformatics*, Chapter 5, Unit 5.6, Wiley, New York.

(40) Verdonk, M. L., Chessari, G., Cole, J. C., Hartshorn, M. J., Murray, C. W., Nissink, J. W., Taylor, R. D., and Taylor, R. (2005) Modeling water molecules in protein-ligand docking using GOLD. *J. Med. Chem. 48*, 6504−6515.

(41) Tyapochkin, E., Cook, P. F., and Chen, G. (2008) Isotope exchange at equilibrium indicates a steady state ordered kinetic mechanism for human sulfotransferase. *Biochemistry 47*, 11894−11899.

(42) Cleland, W. W. (1970) Steady state kinetics. In *The Enzymes Student Edition* (Boyer, P. D., Ed.) pp 1−65, Academic Press, New York.

(43) Lu, L. Y., Hsieh, Y. C., Liu, M. Y., Lin, Y. H., Chen, C. J., and Yang, Y. S. (2008) Identification and characterization of two amino acids critical for the substrate inhibition of human dehydroepian-

drosterone sulfotransferase (SULT2A1). *Mol. Pharmacol. 73*, 660−668.
(44) Chang, H. J., Shi, R., Rehse, P., and Lin, S. X. (2004) Identifying androsterone (ADT) as a cognate substrate for human dehydroepiandrosterone sulfotransferase (DHEA-ST) important for steroid homeostasis: Structure of the enzyme-ADT complex. *J. Biol. Chem. 279*, 2689−2696.
(45) Johnson, K. (1992) Transient-state kinetic analysis of enzyme reaction pathways. In *The Enzymes* (Sigman, D. S., Ed.) pp 1−61, Academic Press, New York.
(46) Xu, Z., Wood, T. C., Adjei, A. A., and Weinshilboum, R. M. (2001) Human 3′-phosphoadenosine 5′-phosphosulfate synthetase: Radiochemical enzymatic assay, biochemical properties, and hepatic variation. *Drug Metab. Dispos. 29*, 172−178.
(47) Klaassen, C. D., and Boles, J. W. (1997) Sulfation and sulfotransferases 5: The importance of 3′-phosphoadenosine 5′-phosphosulfate (PAPS) in the regulation of sulfation. *FASEB J. 11*, 404−418.
(48) Cleland, W. W. (1979) Statistical analysis of enzyme kinetic data. *Methods Enzymol. 63*, 103−138.